A New Look at the Structure and Vibrational Spectra of Small Niobium Clusters and Their Ions

ARTICLE *in* THE JOURNAL OF PHYSICAL CHEMISTRY C · JULY 2010

Impact Factor: 4.77 · DOI: 10.1021/jp103484k

3 AUTHORS, INCLUDING:

Vu Thi Ngan
Quy Nhon University
32 PUBLICATIONS **558** CITATIONS

SEE PROFILE

Minh Tho Nguyen
University of Leuven
748 PUBLICATIONS **10,835** CITATIONS

SEE PROFILE

A New Look at the Structure and Vibrational Spectra of Small Niobium Clusters and Their Ions

Pham Vu Nhat,[†,‡] Vu Thi Ngan,[†] and Minh Tho Nguyen*[,†,§]

Department of Chemistry, Katholieke Universiteit Leuven, B-3001 Leuven, Belgium, Department of Chemistry, Can Tho University, Can Tho, Vietnam, and Institute for Computational Science and Technology of HoChiMinh City, Thu Duc, HoChiMinh City, Vietnam

Received: April 19, 2010; Revised Manuscript Received: June 17, 2010

Geometries, electronic structures, and vibrational spectra of a series of small niobium clusters Nb_n ($n = 2-6$) and their cations and anions are reinvestigated with DFT calculations with cc-pV*a*Z-PP basis sets. CCSD(T) calculations are also carried out for relative energies. In each cluster, different lower lying states are close in energy or quasidegenerate. Stable Nb_n clusters prefer high coordination state and 3D shape. Clusters with an odd number of electrons usually have a doublet ground state (except for Nb_2^+). Neutral and cationic clusters with an even number of electrons tend to possess a triplet ground state, with an exception for Nb_4 (T_d, $^1A_1$). For anions, a competition between low and high spin manifolds is observed. Due to the closed electronic shells, the systems possessing 10 (Nb) and 20 valence electrons (Nb_4) are observed to be more thermodynamically stable than their neighbors. Electron affinities and ionization energies are reevaluated. In particular, new assignments for the vibrational spectra of the Nb_5 and Nb_6 systems are proposed on the basis of a comparison of calculated results with available experimental data.

1. Introduction

There has been continuing interest in the transition metal clusters owing to their potential applications in, among others, electronic devices, nanocatalysis, and medicine.[1] Knowledge of the electronic structure of such clusters provides fundamental insights into their thermal, optical, magnetic, and catalytic properties. Clusters of niobium have thus been the subject of numerous experimental and theoretical investigations. Previous experiments[2−14] mainly dealt with the mass, optical, photoelectron, and infrared spectrometries of small Nb clusters. Knickelbein and Yang[3] measured the ionization energies of Nb_n ($n = 2-76$) using the photoionization efficiency (PIE) technique. Kietzmann et al.[11] recorded the photoelectron spectra (PES) of small Nb_n anions (from 3 to 8 atoms) using a laser vaporization technique, and found that they possess relatively low electron binding energies. The UPE spectra of the larger anions Nb_n^- ($n = 4-200$) were recorded by Wrigge et al.[13] The adiabatic detachment energy of Nb_3^- was evaluated from its 532 nm PE spectrum. James et al.[8] recorded the rotationally resolved electronic spectra of the niobium dimer, whereas Knickelbein and Menezes[5] measured the optical absorption spectra of small and isolated Nb clusters from 7 to 20 atoms from 334 to 614 nm via photodepletion of Nb_n·Ar van der Waals complexes. Recently, Fielicke and co-workers[10] experimentally recorded the far-infrared spectra of both neutral Nb_n and cationic Nb_n^+ clusters ($n = 5-9$) in the region of $85-600$ cm^{-1}.

Theoretical studies on geometries and electronic properties of Nb_n have been performed by several groups,[15−24] using mostly density functional theory (DFT) methods. The optimal geometries and ground states of a series of small clusters ($n = 3-7$) reported in an early investigation by Goodwin et al.[15] suggested that these neutral clusters prefer the lowest possible spin state, except for Nb_2. Subsequent DFT study on $n = 2-23$ species by Kumar and Kawazoe[21] supported this observation. Fowler et al.[19] considered many low-lying states of the cationic and neutral clusters containing three and four niobium atoms using the hybrid functional B3LYP in conjunction with a relativistic compact effective core potential basis set (SBKJ). These authors also used other MO methods such as PMP2, MP4SDQ, CCSD, and CCSD(T). It was concluded that the B3LYP functional gives, in general, the most reliable predictions for both ionization and binding energies. On the contrary, Majumdar and Balasubramanian[22−24] studied the geometries and energy separations of lower lying states of some small niobium clusters using the complete active space multiconfigurational self-consistent field (CASMCSCF) method followed by multireference configuration interaction (MRSDCI) with a 5s/3p/2d basis set. In many cases, the reported MO results[22−24] turned out to disagree with previous DFT data.

As with other transition metal containing compounds, niobium clusters are a rather difficult target for theoretical investigations, in part due to the presence of multiple d electrons and their inherent problems. A crucial problem is that truncated calculations for this type of systems may lead to an incorrect energy ordering of the isomers and electronic states. In addition, the lack of experimental information constitutes another source for uncertainty for spectroscopic parameters. When available, assignment of the experimental data is not straightforward. In principle, the most favored structure of a specific cluster could be identified by comparing the observed properties to the computed counterparts. A number of recent studies have thus combined experiment and theory to acquire comparable spectroscopic information, and thereby led to reliable assignments.[9,10,12,14] However, it appears that the thermodynamically most stable form of a cluster may not be present under the experimental conditions, due to some subtle kinetics. As a consequence,

* To whom correspondence should be addressed. E-mail: minh.nguyen@chem.kuleuven.be.
† Katholieke Universiteit Leuven.
‡ Can Tho University.
§ Institute for Computational Science and Technology of HoChiMinh City.

10.1021/jp103484k
Published on Web 07/16/2010

theoretical results for the lowest lying structure could not match those obtained from measurements. Fielicke et al.[10] assigned the structure for each cluster by a comparison between the observed far-IR spectrum and the calculated ones based on the harmonic vibrational frequencies of different lower lying structural isomers. In the case of Nb_6, either in the neutral or cationic state, the far-IR spectrum of the lowest energy structure determined by DFT calculations does not match the observed one. The spectrum of an energetically higher lying isomer appears to have a better fit, but the assignment was rather tentative. In this context, we set out to have another look at the geometrical and electronic structure of a series of small niobium clusters containing two to six atoms in their neutral, cationic and anionic states. We explore extensively the potential energy surfaces to locate possible new structures, and subsequently compare their calculated IR spectra, electron affinities (EA), and ionization energies (IE) with available experimental data. Our results show agreements but also disagreements with previous studies. The main purpose is thus to propose, where appropriate, new assignments for IR spectra of Nb_n clusters. Finally, we carry out an analysis to gain additional insights into chemical bonding phenomena.

2. Computational Methods

All electronic structure calculations are carried out using the Gaussian 03[26] and Molpro 2009[27] suites of programs. The neutral clusters Nb_n ($n = 2-6$) and their singly charged species are initially investigated by using DFT with the pure BP86 functional and the effective core potential LANL2DZ basis set. Subsequently, geometries of the relevant lower lying isomers are reoptimized utilizing the correlation consistent cc-pV*a*Z-PP (a = D, T, Q) basis sets[28−30] with the exchange-correlation functionals B3LYP, BLYP, BP86, and BPW91. PP stands for an effective core potential (ECP), in which the electrons in the inner shells along with the nucleus are considered as the inert core, and the $(n-1)$s, $(n-1)$p, $(n-1)$d, ns, and np orbitals of the atom are taken as valence orbitals. The interaction between valence electrons and inert core is included in the pseudopotential. This allows us to reduce substantially the number of electrons to be treated, and thereby computing times. For each cluster, we consider the two lowest spin states. Harmonic vibrational frequencies are used to characterize the stationary points and to simulate the vibrational spectra (without scaling). The coupled-cluster theory CCSD(T) method in conjunction with the cc-pVTZ-PP basis set is also used for the equilibrium distance and energies of the dimer and its singly charged clusters. For larger systems, only single point energy CCSD(T) calculations are calculated at the BPW91/cc-pVTZ-PP optimized geometries. In the coupled-cluster computations, the core orbitals are fronzen, and the restricted HF-unrestricted CC formalism, R/UCCSD(T), is applied for open-shell systems.

3. Results and Discussion

Cartesian coordinates of the optimized geometries, total energies, and shapes of molecular orbitals are given in the Supporting Information. We first examine the geometries, electronic states and energetic parameters of the lower lying isomers, followed by an assignment of the IR spectra. The electronic distribution and bonding are discussed in the next section. Figure 1 summarizes the characteristics of the structures considered including their shapes, symmetry point groups, and electronic states.

3.1. Equilibrium Structures. ***A. The Dimers.*** Nb_2 and its ions have been extensively investigated in previous studies.[8,15,20]

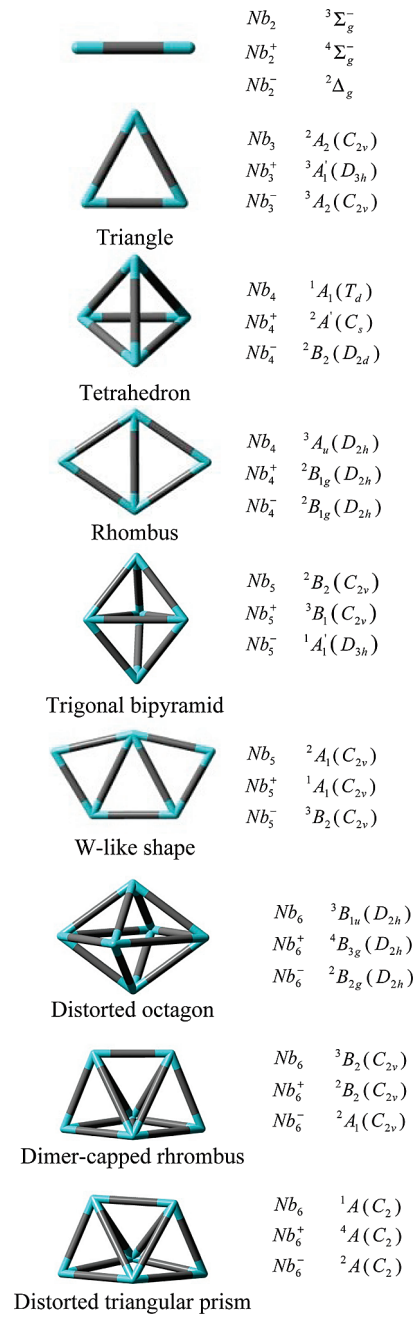

Figure 1. Selected structures of the ground state and low-lying states of $Nb_n^{0,\pm1}$ (at the BPW91/cc-pVTZ-PP level).

Let us recall the main properties. The orbital configuration of Nb_2 is $...\pi_g^4 1\sigma_g^2 2\sigma_g^2 \delta_g^2$ where the two unpaired electrons occupy the doubly degenerate δ_g orbital. Such occupancy gives rise to three possible states $^1\Sigma_g^+$, $^3\Sigma_g^-$, and $^1\Gamma_g^-$, in which the $^3\Sigma_g^-$ state is confirmed to be the lowest energy. For the purpose of calibration, the bond length of the neutral dimer is computed by using four different DFT functionals and the CCSD(T) method in conjunction with the cc-pV*a*Z-PP basis sets (a = D, T, and Q). These parameters are only slightly modified with respect to the basis sets. By using the cc-pVQZ-PP basis set, the Nb_2 ($^3\Sigma_g^-$) bond distance amounts to 2.062 (B3LYP), 2.099 (BLYP), 2.082 (BP86), 2.081 (BPW91), and 2.119 Å (CCSD(T)), which can be compared with the experimental value of 2.078 Å.[8] The $^1\Sigma_g^+$ is the lowest singlet excited state with a gap of ~0.30 eV by BPW91, which is larger than those of 0.1−0.2 eV previously obtained with FOCI- FO(MR)CI techniques.[20]

For the cation, the $^4\Sigma_g^-$ state associated with the orbital configuration $\pi_g^4 1\sigma_g^2 \delta_g^2 2\sigma_g^1$ is confirmed to be the ground state, with the low spin state $^2\Gamma_g$ being 0.29 (BPW91) or 0.32 eV (CCSD(T)) above it. Removal of an electron from Nb_2 ($^3\Sigma_g^-$) to form the $^4\Sigma_g^-$ cation unexpectedly shortens the equilibrium distance to 2.040 Å (BPW91).

The anion properties are more sensitive with the methods employed. The B3LYP, BLYP, and BP86 functionals yield a preference of a low-spin Nb_2^-. It has a shorter distance in comparison with the neutral since one electron is added to the bonding δ_g MO. The ground state configuration of Nb_2^- thus contains three electrons on the doubly degenerate orbital δ_g, which gives rise to a single term $^2\Delta_g$. However, the functional BPW91 predicts that $^2\Delta_g$ state to be ~0.05 eV above the higher spin $^4\Sigma_u^-$ state ($1\sigma_g^2\pi_g^4 2\sigma_g^2\delta_g^2\sigma_u^1$), with a longer bond length than that of the neutral, due to the occupancy of an antibonding MO. CCSD(T)/cc-pVTZ-PP calculations indicate that the quartet state is only 0.03 eV higher than the doublet state. Within the expected accuracy of these methods, both high- and low-spin anionic states can be regarded as nearly degenerate.

The bond length and vibrational frequency of Nb_2 at the different levels of theory are summarized in Table S3 of the Supporting Information, along with experimental values. In general, the employed DFT methods predict bond lengths with acceptable agreement with experiment. The B3LYP functional consistently predicts the shortest equilibrium (r_e) distance. The others somehow overestimate it. With the same basis set, the predicted bond length increases in the order B3LYP < BP86, BPW91 < BLYP. As expected from the calculated bond lengths, the predicted vibrational frequencies decrease in the order B3LYP > BP86, BPW91 > BLYP, but all functionals likely overestimate this parameter. It is, however, difficult to conclude which functional provides the best results since the experimental distance is the vibrationally averaged (r_0) value, and only one comparison can actually be made. In spite of the limited data, both pure BP86 and BPW91 functionals are chosen for further studies.

B. The Trimers. The electronic state of Nb_3 remains a matter of discussion. Kietzmann et al.[11,12] and Fournier et al.[18] used DFT methods and agreed with each other that the trimer anion Nb_3^- exhibits a D_{3h} shape and a singlet ground state. On the contrary, Majumdar and Balasubramanian[23] found that the lowest energy structure of the triatomic anion is an isosceles triangle (C_{2v}) with a high spin ground state $^3A_2$ at the B3LYP level, but a low spin $^1A_1$ state at a MRSDCI level. The latter authors[23] also concluded that the ground state of Nb_3 is the $^2B_1(C_{2v})$ state at both levels. However, this disagreed with earlier DFT results of Goodwin et al.[15] and Kumar et al.[21] that showed a $^2A_2$ ground state for Nb_3. Recently, Zhai et al.[14] used B3LYP calculations in conjunction with a 14-electron pseudopotential plus a valence basis set augmented with two f-type and one g-type polarization functions, and also obtained a $^3A_2(C_{2v})$ ground state for Nb_3^-. At the same level, the distorted $^2A''(C_s)$ triangular structure was found for the ground state of Nb_3.[14]

Indeed, we find that the identity of the triatomic entities is strongly dependent on the method employed. The pure BLYP, BP86, and BPW91 functionals predict a $^2A_2$ ground state for the C_{2v} isosceles triangle Nb_3, with two long plus one short bonds. The B3LYP is confirmed to predict a $^2B_1$ ground state, arising also from an isosceles triangle but with two short plus one long bonds. Both $^2A_2$ and $^2B_1$ states are in fact the two resulting components of Jahn−Teller distortions from the unstable degenerate $^2E''(D_{3h})$ state following two distinct (perpendicular) vibrational modes. R/UCCSD(T)/cc-pVTZ-PP calculations for both Nb_3 structures point out that the $^2A_2$ state is 0.11 eV lower in energy than the $^2B_1$ counterpart. To probe further its identity, we separately construct the multiconfigurational CASSCF(15,14)/ANO-RCC[31] wave functions, followed by second-order perturbation CASPT2 for both doublet states. The inactive space of Nb_3 consists of the 22 a_1, 9 b_1, 6 a_2, and 17 b_2 orbitals. Fifteen valence electrons then have variable occupancy in an active space of 14 orbitals including 7 a_1, 3 b_1, 2 a_2, and 2 b_2 orbitals. At this level, the $^2A_2$ state remains favored by ~0.33 eV over the $^2B_1$ counterpart. In spite of the small separation between both states, our results suggest that the $^2A_2$ state, whose leading orbital configuration is $a_1^2 b_1^2 a_1^2 b_2^2 a_1^2 a_2^1 a_1^2 b_1^2$, constitutes the electronic ground state of Nb_3.

Concerning Nb_3^-, DFT calculations suggest that the most stable form of Nb_3^- is an isosceles triangle (C_{2v}) with a $^3A_2$ state.[23] In an D_{3h} form, the corresponding singlet state $^1A_1'$: $...(e')^4(a_1')^2(e'')^4$ is not subjected to a Jahn−Teller distortion, but this $^1A_1'$ state is located 0.19 eV higher than the triplet state (BPW91). On the contrary, CCSD(T) single point calculations reverse the state ordering in predicting that the singlet state is ~0.6 eV lower than the triplet. In other words, our results concur with those reported in ref 23 using MO methods. We thus would suggest that the Nb_3^- anion possesses a high-symmetry low-spin ground state $^1A_1'(D_{3h})$.

For Nb_3^+, the most favorable form is an equivalent triangle (D_{3h}) in which the high-spin state has the orbital configuration $^3A_1'$: $...(e')^4(a_1')^2(e'')^2$. Pairing the two unpaired electrons in one orbital e'' reduces the symmetry by the Jahn−Teller effect, but this brings no benefit in terms of energy. Actually, the $^1A_1$ state of an isosceles triangle (C_{2v}) is ~0.4 eV less favored than the $^3A_1'$ state (BPW91). This is in line with previous findings by Fowler and co-workers.[19] These results, however, disagreed with the B3LYP data reported in ref 22, in that the most stable form of Nb_3^+ has a $^3B_1$ state (C_{2v}). In this work, we find that $^3B_1$ is an excited state, being 0.15, 0.18, and 0.40 eV above the $^3A_1'$ state by B3LYP, BPW91, and CCSD(T) calculations, respectively.

Figure 2 shows the vibrational spectra computed at the BPW91/cc-pVTZ-PP level for some lower lying trimeric forms. No experimental IR spectrum is available for this system. The predicted spectrum of the $^2A_2$ neutral ground state contains two distinct peaks centered at ~140 and 240 cm^{-1}. The spectrum of the D_{3h} cation becomes much simpler, with a doubly degenerate mode at ~240 cm^{-1}. The anion in D_{3h} symmetry with the state $^1A_1'$ also contains a doubly degenerate mode at ~225 cm^{-1}. Thus there is a typical peak of the trimer in the range of 225−240 cm^{-1}.

C. The Tetramers. In agreement with previous studies,[15,19,21] a tetrahedral $^1A_1(T_d)$ structure is the lowest-energy isomer of Nb_4. This neutral also exists as a rhombus (D_{2h}) but both corresponding states ^3A_u and ^1A_g are 0.73 and 0.83 eV, respectively, higher in energy than the ground state (BPW91). The rhombus form is a higher energy local minimum of the cation and anion as well. Their relative energies can be seen in Table 1.

For Nb_4^+ and Nb_4^-, results reported in the literature are not consistent with each other. Both HOMO and LUMO of Nb_4 are degenerate, so attachment or removal of an electron reduces the symmetry because of a Jahn−Teller effect. The ground state of Nb_4^+ ranges from an ideal to a distorted tetrahedron having either a $^2A_1(C_{2v})$ or $^2A'(C_s)$ state.[19,22] Our calculations reveal that the cation prefers a distorted tetrahedron with a D_{2d} point group and a $^2B_2$ state. Using the BPW91 functional, we find that Nb_4^+ is marginally more stable in a lower symmetry form (C_s, $^2A'$). The $^2A_1$ (C_{2v}) structure is a transition structure with

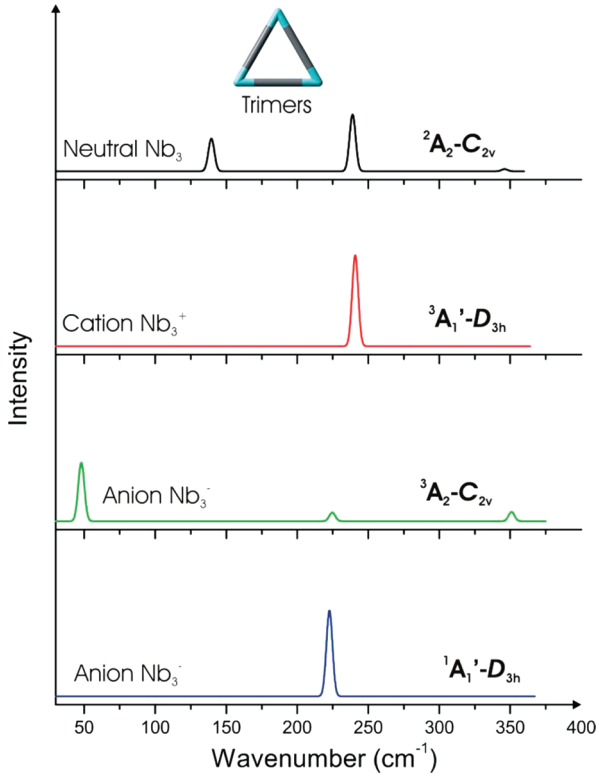

Figure 2. IR spectra of trimer clusters.

a small imaginary frequency of 92*i* cm^{-1}. The other component $^2B_2$ of the geometrical distortion from the D_{2d} structure is also a transition structure with a comparable imaginary frequency. Nevertheless, the three states $^2A'$, $^2B_2$, and $^2A_1$ are nearly identical in terms of energy at the BPW91 and CCSD(T) levels. Previous CASMCSCF and MRSDCI calculations[22] also suggested that the lowest lying geometry of Nb_4^+ is a C_s pyramid ($^2A'$). The other isomer of Nb_4^+ is a rhombus (D_{2h}, $^2B_{1g}$), which is 0.71 and 0.81 eV less stable than the ground state at the BPW91 and CCSD(T) methods, respectively. In this context, the $^2A'$ state appears to be the ground state of the tetraatomic cation.

Similarly, the identity of the ground state of the anion Nb_4^- is still not clear. Earlier DFT-LSD calculations[11] predicted that this is a low-spin distorted tetrahedron. Subsequent computational studies[24] suggested a pyramidal form (C_s, $^2A'$) at the B3LYP level, but a rhombus form (D_{2h},$^2B_{3g}$) at a MRSDCI level. The lower lying electronic states and structures obtained for Nb_4^- with BPW91 are listed in Table 1. Our results show that the anion is stable in either a distorted tetrahedral geometry (D_{2d}, $^2B_2$) or a distorted structure (C_s, $^2A''$), with the same energy content. The gap between the two forms is in fact negligible, ~0.007 eV. The potential energy surface in this region is quasi-flat. Another local minimum of Nb_4^- is a rhombus (D_{2h}, $^2B_{1g}$) but at 0.28 eV higher energy. CCSD(T) single point calculations with BPW91 geometries confirm the energy ordering but increase this gap to 0.35 eV. It can thus be concluded that the anion Nb_4^- exhibits a $^2B_2$ ground state, but with a highly fluxional structure.

The vibrational spectra for tetramers are depicted in Figure 3. The neutral spectrum is simple with a triply degenerate mode centered at ~245 cm^{-1}. The cation contains two peaks in the range 230−240 cm^{-1} and a very low intensity peak at ~100 cm^{-1}. The anion also has the distinct band around 240 cm^{-1}. No experimental IR data are actually available for the four niobium species.

TABLE 1: Ground States and Low-Lying States of $Nb_n^{0,\pm1}$ (n = 2−6) at the BPW91/cc-pVTZ-PP Level

cluster	geometry	symmetry	state	RE (eV)
Nb_2	linear	$D_{\infty h}$	$^3\Sigma_g^-$	0.00
			$^1\Sigma_g^+$	0.37
Nb_2^+	linear	$D_{\infty h}$	$^4\Sigma_g^-$	0.00
			$^2\Gamma_g$	0.27
Nb_2^-	linear	$D_{\infty h}$	$^4\Sigma_u^-$	0.00
			$^2\Delta_g$	0.05
Nb_3	isosceles triangle	C_{2v}	$^2A_2$	0.00
			$^4A_2$	0.52
Nb_3^+	equivalent triangle	D_{3h}	$^3A_1'$	0.00
	isosceles triangle	C_{2v}	$^3B_1$	0.18
			$^1A_1$	0.40
Nb_3^-	isosceles triangle	C_{2v}	$^3A_2$	0.00
	equivalent triangle	D_{3h}	$^1A_1'$	0.19
Nb_4	tetrahedron		$^1A_1$	0.00
	rhombus	D_{2h}	^3A_u	0.73
			^1A_g	0.83
Nb_4^+	distorted tetrahedral	C_s	$^2A'$	0.00
		C_{2v}	$^4A_2$	0.72
	rhombus	D_{2h}	$^2B_{1g}$	0.71
			^4A_u	1.32
Nb_4^-	distorted tetrahedral	D_{2d}	$^2B_2$	0.00
		C_s	$^2A''$	0.007
		C_{2v}	$^4A_2$	0.34
	rhombus	D_{2h}	$^2B_{1g}$	0.28
			$^4B_{2g}$	0.70
Nb_5	distorted trigonal bipyramid	C_{2v}	$^2B_2$	0.00
			$^4B_1$	0.39
		C_s	$^4A'$	0.23
	W-like shape	C_{2v}	$^2A_1$	1.84
Nb_5^+	distorted trigonal bipyramid	C_{2v}	$^3B_1$	0.00
			$^3A_1$	0.001
			$^1A_1$	0.13
		C_s	$^1A'$	0.18
	W-like shape	C_{2v}	$^1A_1$	2.02
Nb_5^-	trigonal bipyramid	D_{3h}	$^1A_1'$	0.00
	distorted trigonal bipyramid	C_{2v}	$^3A_2$	0.18
	W-like shape	C_{2v}	$^3B_2$	1.69
Nb_6	dimer-capped rhombus	C_{2v}	$^3B_2$	0.00
			$^1A_1$	0.13
	distorted triangular prism	C_2	^1A	0.08
	distorted octagon	D_{2h}	$^3B_{1u}$	0.14
			^1A_g	0.31
		D_{4h}	$^3A_{1g}$	0.24
Nb_6^+	dimer-capped rhombus	C_{2v}	$^2B_2$	0.00
			$^4B_1$	0.22
	distorted octagon	D_{2h}	$^2B_{3u}$	0.04
			$^4B_{3g}$	0.10
			$^2B_{2g}$	0.33
	distorted triangular prism	C_2	^4A	0.29
Nb_6^-	distorted triangular prism	C_2	^2A	0.00
	dimer-capped rhombus	C_{2v}	$^2A_1$	0.01
			$^4A_2$	0.13
	distorted octagon	D_{2h}	$^2B_{2g}$	0.19

D. The Pentamers. Previous DFT calculations agreed with each other that the ground state of Nb_5 has a distorted trigonal bipyramid shape with C_{2v} point group and a low spin. Our findings concur with this, and show in addition that the ground $^2B_2$ state is below the lowest quartet $^4A'$ state (C_s) by 0.23 (BPW91) to 0.53 eV (CCSD(T)). Another Nb_5 isomer, which has a planar W-type shape (C_{2v}, $^2A_1$), is 1.84 eV above the ground state (Table 1).

For the cations, however, previous results are again not consistent. For Nb_5^+, MCSCF calculations[22] indicated a low-spin distorted edge-capped tetrahedron (C_s, $^1A'$) to be the most favored isomer. On the contrary, B3LYP calculations[10] pointed toward a triplet distorted trigonal pyramide (C_{2v}, $^3A_1$).

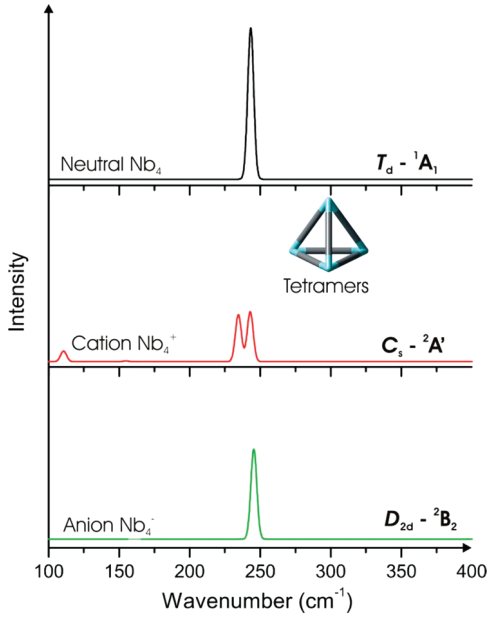

Figure 3. IR spectra of tetramer clusters.

Our BPW91 results indicate that the most stable form of Nb_5^+ is a distorted trigonal pyramid (C_{2v}), but both high spin $^3B_1$ and $^3A_1$ states are quasi-degenerate, with a tiny energy difference of 0.001 eV (Table 1). The corresponding low spin states $^1A'$ (C_s) and $^1A_1$ (C_{2v}) are located at 0.18 and 0.15 eV above the $^3B_1$ state (BPW91). However, CCSD(T)/BPW91 calculations reverse the energy ordering, in that the $^1A_1$ (C_{2v}) state now becomes the lowest-lying state. The other states $^3B_1$, $^3A_1$, and $^1A'$ are calculated at 0.09, 0.11, and 0.33 eV, respectively, above $^1A_1$. In this context, we would suggest that Nb_5^+ is characterized by a singlet ground state, but with a tiny triplet−singlet separation gap.

The ground state of the anion Nb_5^- was found to be either a singlet high-symmetry trigonal bipyramid (D_{3h}),[11] a distorted trigonal bipyramid with a low spin state (C_{2v}, $^1A_1$) (by B3LYP), or a high spin ground $^3B_1$ state when employing CASMCSCF calculations.[24]

Our BPW91 results predict the high-symmetry low-spin (D_{3h}, $^1A_1'$) as the most stable form of Nb_5^-. The orbital configuration of Nb_5^- related to the state $^1A_1'$: $...(e')^4(a_1')^2(a_2'')^2(e'')^4$ is stable with respect to a Jahn−Teller effect. We are not able to locate a $^1A_1$ (C_{2v}) state, as all geometry optimizations invariably converge to the $^1A_1'$ (D_{3h}) state. The high spin $^3A_2$(C_{2v}) state is an excited state at 0.18 eV higher energy. At the CCSD(T) level, the singlet−triplet separation is significantly reduced, with the $^1A_1'$ (D_{3h}) state being only 0.04 eV more stable than the $^3A_2$ (C_{2v}) state. These results again suggest that the Nb_5^- anion exhibits a nearly degenerate ground state in both singlet and triplet manifolds.

Figures 4 and 5 compare the theoretical and experimental vibrational spectra of the pentamers. The experimental spectra were reported by Fielicke and co-workers.[10] The calculated vibrational spectrum of Nb_5 ($^2B_2$) covers the range below 300 cm^{-1} with three specific peaks, where the most intense one is centered at around 175 cm^{-1}, which is in line with experimental results (Figure 4). For the purpose of comparison, the calculated spectra of both states of the anion are also plotted in Figure 4. The vibrational features are thus much modified upon electron addition.

For the cation, its far-IR spectrum contains distinct bands in the range from 150 to 400 cm^{-1} in which the peak at ~280 cm^{-1}

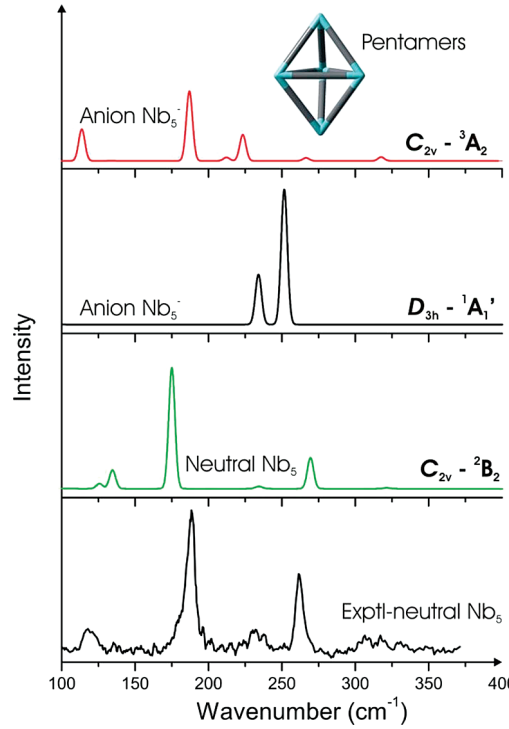

Figure 4. Experimental and theoretical IR spectra of Nb_5 and theoretical IR spectra of Nb_5^-.

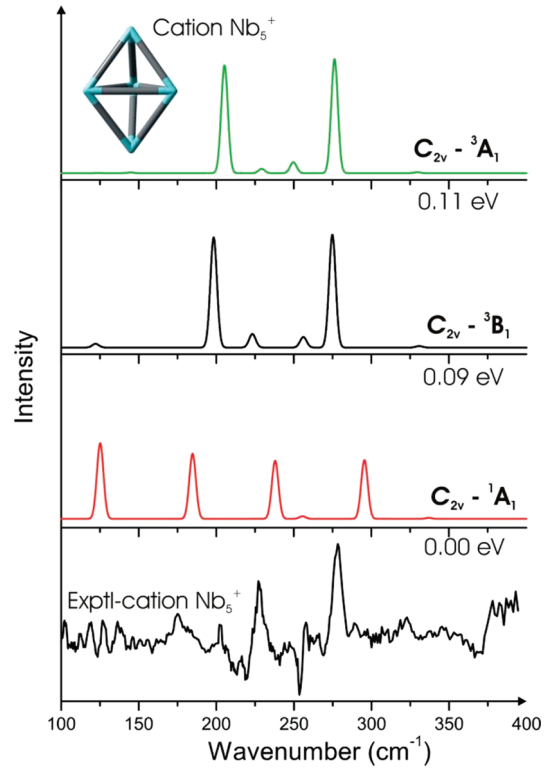

Figure 5. Experimental and theoretical IR spectra of Nb_5^+.

is the most typical one (Figure 5). In view of the near degeneracy of states under C_{2v}, the IR spectra of the three $^1A_1$, $^3B_1$, and $^3A_1$ states are compared in Figure 5. There is a peak in each of these spectra corresponding to the observed peak at 280 cm^{-1}. The $^1A_1$ spectrum also covers the range from 100 to 300 cm^{-1}, where the distinct band of ~230 cm^{-1} was also detected experimentally. These facts suggest that a mixture of these lowest-lying states is actually manifested in the observed IR spectrum.

TABLE 2: Ground State and Low-Lying States of $Nb_6^{0,\pm1}$ (CCSD(T)/cc-pVTZ-PP Single Point Calculations at the BPW91/cc-pVTZ-PP Geometries)

cluster	geometry	symmetry	state	rel energy (eV)
Nb_6	distorted octagon	D_{2h}	$^3B_{1u}$	0.00
			^1A_g	0.001
	dimer-capped rhombus	C_{2v}	$^3B_2$	0.21
			$^1A_1$	0.31
	distorted triangular prism	C_2	^1A	0.34
	distorted octagon	D_{4h}	$^3A_{1g}$	0.99
Nb_6^+	dimer-capped rhombus	C_{2v}	$^2B_2$	0.00
			$^4B_1$	0.36
	distorted octagon	D_{2h}	$^4B_{3g}$	0.12
			$^2B_{3u}$	0.18
			$^2B_{2g}$	0.32
	distorted triangular prism	C_2	^4A	0.60
Nb_6^-	distorted octagon	D_{2h}	$^2B_{2g}$	0.00
	dimer-capped rhombus	C_{2v}	$^2A_1$	0.14
			$^4A_2$	0.25
	distorted triangular prism	C_2	^2A	0.16

E. The Hexamers. Previous theoretical studies on the $Nb_6^{0/\pm1}$ system were mainly based on DFT calculations using different functionals, and the identity of the most stable structures remains a matter of debate. For the neutral, Goodwin et al.[15] reported a dimer-capped rhombus to be the lowest-energy form. Conversely, Kumar et al.[21] suggested a distorted triangular prism associated with a singlet state. Fielicke et al.[10] predicted two isoenergetic isomers including a singlet distorted triangular prism (C_2) and a triplet tetragonal-square bipyramid (or distorted octagon, D_{4h}).

Our present DFT/BPW91 results point toward a dimer-capped C_{2v} rhombus with a high spin $^3B_2$ state as the lowest energy structure. The corresponding low spin $^1A_1$ state of such a form is energetically less favorable by 0.13 eV, and has in addition an imaginary frequency of $70i$ cm^{-1}. The second most stable structure is a distorted triangular prism (C_2) but it prefers to stay in a low spin ^1A state, and is only 0.08 eV above the ground state. Another structure obtained for Nb_6 is a distorted D_{2h} octagon. In this shape, the $^3B_{1u}$ state is more stable than the ^1A_gcounterpart (Figure 1). Their relative energies to the ground state amount to 0.14 and 0.31 eV, respectively. The high symmetry D_{4h} structure with a triplet state $^3A_{1g}$, which was reported in ref 10, is 0.24 eV above the ground state and has in addition a small imaginary frequency of $50i$ cm^{-1}.

Let us remind that all results mentioned above are obtained with BPW91/cc-pVTZ-PP computations. In this case, CCSD(T)/cc-pVTZ-PP single point calculations reveal a different energy landscape (Table 2). The distorted high spin octagon (D_{2h}, $^3B_{1u}$) becomes now the lowest energy structure, which is, however, quasi-isoenergetic with the corresponding ^1A_g state of this geometry. The dimer-capped rhombus (C_{2v}, $^3B_2$) state is now 0.21 eV higher in energy than the ground state. Detailed information on these electronic states is given in Table 2. It appears again that the neutral hexamer Nb_6 is characterized by distorted octagon with quasi-degenerate singlet and triplet ground states.

Previous results obtained for the Nb_6^+ cation again disagreed with each other on its ground state. Local spin density calculations[15] identified its lowest energy form to be a doublet dimer-capped rhombus. Subsequent DFT computations[10] assigned a doublet D_{2h} structure as the most stable isomer. Our BPW91 calculations given in Table 1 suggest that the lowest energy isomer of Nb_6^+ is indeed a dimer-capped rhombus having a C_{2v} geometry and a low spin $^2B_2$ state. The higher spin state $^4B_1$ of this shape is at 0.22 eV above. Nevertheless, a tetragonal bipyramid (D_{2h}, $^2B_{3u}$) turns out to be less favored by only 0.04 eV. The isomer bearing a tetragonal bipyramid with a high spin state $^4B_{3g}$ is 0.10 eV higher than the ground state.

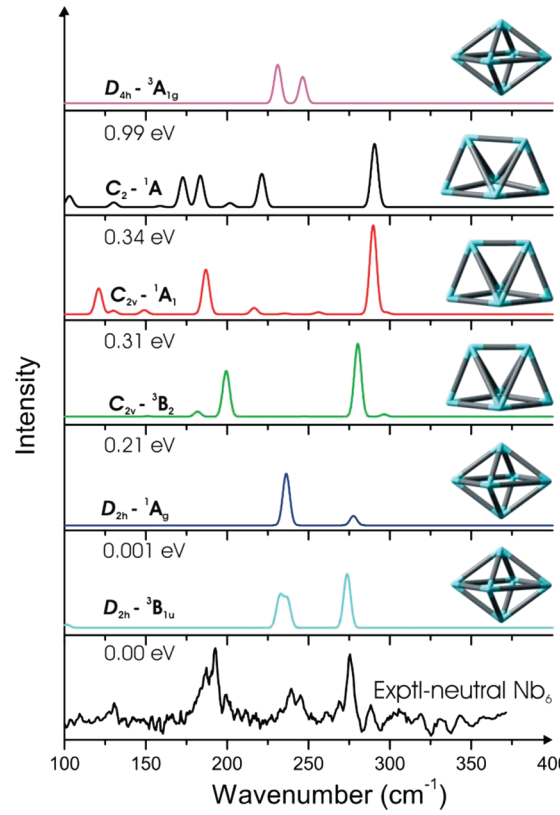

Figure 6. Experimental and theoretical IR spectra of Nb_6.

CCSD(T) calculations support the DFT-based observations above, confirming the dimer-capped rhombus structure (C_{2v}, $^2B_2$) as the ground electronic state of Nb_6^+. The next lower lying state is the $^4B_{3g}$ of a tetragonal bipyramid (D_{2h}), which lies at 0.12 eV higher energy (see Table 2).

BPW91 results point out that a distorted triangular prism (C_2, ^2A) is the lowest energy structure of the hexaatomic anion. This is in agreement with previous local spin density calculations.[11,18] The dimer-capped rhombus structure (C_{2v}, $^2A_1$) is only 0.01 eV higher but it possesses a tiny imaginary frequency of $50i$ cm^{-1}. The anion has also another local minimum, which is a distorted D_{2h} octagon with a $^2B_{2g}$ state and 0.19 eV less stable than the C_2 form. However, this energy ordering is actually reversed by CCSD(T)/cc-pVTZ-PP calculations (Table 2). Accordingly, the most stable form of Nb_6^- is now the distorted octagon (D_{2h}, $^2B_{2g}$) structure. Relative to the latter, the states ^2A (C_2) and $^2A_1$ (C_{2v}) are calculated at 0.16 and 0.14 eV higher, respectively (CCSD(T) values).

The shapes and IR spectra of some low-energy structures of both Nb_6 and Nb_6^+ determined with BPW91/cc-pVTZ-pp calculations are shown in Figures 6 and 7, along with the experimental spectra taken from ref 10. For both neutral and cationic species, our assignments are at variance with those proposed by Fielicke et al.[10] These authors assigned the C_2 (^1A) structure as the carrier for the observed spectrum (Figure 6). For the neutral, we find that the distorted high spin octagon (D_{2h}), either in the triplet $^3B_{1u}$ or singlet ^1A_g state, exhibits two distinct bands centered at around 230 and 275 cm^{-1}, but with different intensities. Both bands are seen in the experimental spectrum (Figure 6). On the contrary, the dimer-capped rhombus with a triplet state (C_{2v}, $^3B_2$) has two intense peaks at 200 and

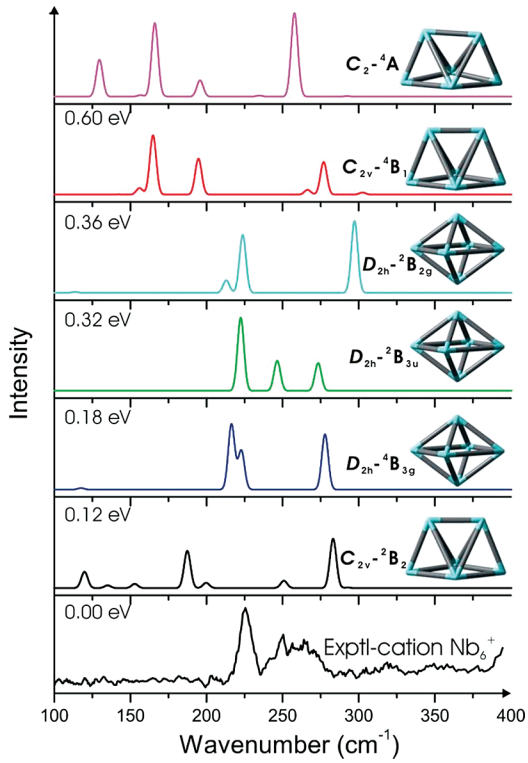

Figure 7. Experimental and theoretical IR spectra of Nb_6^+.

TABLE 3: Adiabatic Electron Affinities (ADE) and Vertical Detachment Energies (VDE) of Nb_n^- ($n = 2-6$) Clusters (BPW91/cc-pVTZ-PP)

reaction	ADE	VDE	exptl (eV)[a]
$Nb_2^-(^4\Sigma_u^+) \rightarrow Nb_2$	0.82	0.83	
$Nb_3^-(^3A_2) \rightarrow Nb_3$	0.98	1.03	1.09
$Nb_4^-(^2B_2) \rightarrow Nb_4$	0.83	0.86	1.10
$Nb_5^-(^1A_1') \rightarrow Nb_5$	1.38	1.48	1.52
$Nb_6^-(^2A) \rightarrow Nb_6$	1.36	1.50	1.58

[a] Kietzmann, H.; Morenzin, T.; Bechthold, P. S.; Gantefor, G.; Eberhardt, W.; Yang, D.-S.; Hackett, P. A.; Fournier, R.; Pang, T.; Chen, C. *Phys. Rev. Lett.* **1996**, *77*, 4528.

280 cm^{-1}, the lower frequency of the two peaks is not present in the two lower lying states, but is also observed in the experimental spectrum. Hence, it can be deduced that the measured spectrum likely arises from a superposition of the spectra of three states rather than from a sole carrier.

For Nb_6^+, Fielicke et al.[10] assigned the $^4B_1$ (C_{2v}) structure to be responsible for the observed spectrum (Figure 7), even though this structure is not the most stable form. As discussed above, both BPW91 and CCSD(T) calculations predict the dimer-capped rhombus with a doublet state (C_{2v}, $^2B_2$) to be the most stable isomer. However, its calculated IR spectrum does not match experiment well. Instead, the vibrational spectra of the distorted octagon in both low $^2B_{3u}$ and high spin $^4B_{3g}$ states better reproduce the experimental spectra, in particular the low spin structure (Figure 7). We would suggest that the neutral Nb_6 represents another case in which the lowest lying isomer is not responsible for the observed IR spectrum. Under experimental conditions, higher lying isomers were present and turned out to be its carrier. For the sake of completeness, the IR spectra of the anion are given in the Supporting Information.

3.2. Electron Affinities and Ionization Energies. Table 3 lists the adiabatic electron affinities (ADE) and vertical detachment energies (VDE) of the six niobium anionic clusters considered at different calculations. In practice, the ADE of an anion is less available than its VDE, which is more commonly determined. By employing photoelectron spectroscopy techniques, Kietzmann and co-workers[11] evaluated the VDEs for the small Nb_n^- ($n = 3-8$) clusters. Theoretical and experimental VDEs are compared in Table 3. Calculations carried out with the B3LYP, BLYP, BP86, and BPW91 functionals and the cc-pV*a*Z-PP basis sets are given in the Supporting Information.

Overall, the calculated VDEs increase monotonously according to the cluster size, except for the tetramer. This can deduce that removal of one electron from Nb_4^- to form Nb_4 is easier than the same process from Nb_3^-, Nb_5^-, and Nb_6^-. The neutral tetramer is somewhat more stable than its neighbors, since its electronic structure corresponds to a magic number of 20 valence electrons, according to the phenomenological shell model.

Of the four functionals considered, the BPW91 provides us with more reliable values for this quantity. The VDEs increase in the following order, BP86 > BPW91 ≈ experimental values. To some extent, it is rather difficult to evaluate this property as the added electron in the anion tends to move far away from the nuclei, and thereby makes it different from the neutral one, and as a consequence induces a certain imbalance in the theoretical treatment. Nevertheless, the calculated values given in Table 3 are in good agreement with the measured values.

TABLE 4: Theoretical and Experimental Ionization Energies of Nb_n (cc-pVTZ-PP)

	BP86		BPW91		
reaction	AIE	VIE	AIE	VIE	exptl[a] (eV)
$Nb_2(^3\Sigma_g^-) \rightarrow Nb_2^+$	6.47	6.50	6.26	6.29	$6.20^{+0.1}_{-0.0}$
$Nb_3(^2A_2) \rightarrow Nb_3^+$	5.88	6.01	5.72	5.86	5.81 ± 0.05
$Nb_4(^1A_1) \rightarrow Nb_4^+$	5.74	5.85	5.56	5.66	5.64 ± 0.05
$Nb_5(^2B_2 \rightarrow Nb_5^+$	5.44	5.45	5.25	5.27	5.45 ± 0.05
$Nb_6(^3B_2) \rightarrow Nb_6^+$	5.38	5.46	5.22	5.30	5.38 ± 0.05

[a] Knickelbein, M. B.; Yang, S. *J. Chem. Phys.* **1990**, *93*, 5760.

Table 4 lists the calculated vertical and adiabatic ionization energies (IE) of Nb_n clusters. The values obtained with four functionals are given in the Supporting Information. In fact, they give a similar trend, i.e. the IEs decrease monotonously with the increasing size of clusters. Knickelbein and Yang[3] determined the IEs of Nb_n ($n = 2-76$) using photoionization efficiency (PIE) spectrometry. Such experimental values are vertical in nature, and hence can be best approximated by calculated vertical ionization energy (VIE) from the corresponding neutral. The VIEs of Nb_n ($n = 2 - 6$) listed in Table 4 are in good agreement with experiment.

Several groups investigated the IEs of Nb_n. However, the reported results appear to be underestimated with respect to experimental values. For example, CISD calculations[3] yielded the IEs of 4.85, 4.33, and 4.31 eV for Nb_2, Nb_3, and Nb_4, respectively. These are substantially smaller than the measured values given in Table 4. MRSDCI[20] and DFT[15] derived a value of around 5.90 eV for the IE of Nb_2 (exptl: 6.20 eV). When performing the MRSDCI+Q calculations, the IE of Nb_2 is improved, being 0.1 eV lower than the experimental value.

3.3. Molecular Orbital Analyses. The density of states (DOS) of a system refers to the number of states at each energy level that are available to be occupied. The DOS of electrons in a molecular system describes the energy spectrum of its molecular obitals. Electron density of states computed from a specific orbital is called the partial density of states (pDOS). The density of states can be used to assign the contribution of atomic atoms to a particular molecular orbital.[32,33] The DOS graphics are plotted with the PyMolyze-2.0 program.[34] Figure

S2 of the Supporting Information illustrates the total and partial DOS of Nb_2. It is clear that d orbitals and s orbitals mostly contribute to forming molecular orbitals in the valence band. The orbitals $1\sigma_g$ and $2\sigma_g$, whose energies are around −4.9 and −4.1 eV, are formed by overlap of atomic orbitals $4d_{z^2}$ and 5s. Hence, they are higher in energy than the π_u orbitals, which are combined from orbitals $4d_{yz}$ and $4d_{xz}$.

Figure S3 and S4 of the Supporting Information display the shape of frontier molecular orbitals in the ground state of $Nb_n^{0,\pm1}$ and their energy gaps. This gap provides an important insight into their kinetic stability. It also reflects the ability to stimulate electrons from occupied orbitals to virtual orbitals. A large gap is a good indicator of the cluster inertia, or lower chemical activities. The HOMO-LUMO gaps of Nb_2 and Nb_4 are much larger than those of the others, implying a relatively higher stability of these clusters compared to their neighbors.

The stepwise dissociation energies $D_e(Nb_n)$ have been measured by Armentrout and co-workers[2] for the series $n = 2-6$ using the collision induced dissociation (CID) method. The D_e value of Nb_4 is indeed the highest among these clusters. Our calculations using both DFT and CCSD(T) methods also support this trend (results are given in Figure S6 of the Supporting Information). An understanding of these observations can be based on the electron shell model,[25] which predicts that spherical clusters are magic if they hold the number of valence electrons corresponding to the closed shell in the sequence (1S/1P/1D/2S/1F...). In the cases of Nb_2 and Nb_4, since their shapes are not perfect spheres, the energy levels of the shells are reversed. As a result, the shell sequences become $1S^2/2S^2/1P^6$ for Nb_2 and $1S^2/2S^2/1D^{10}/1P^6$ for Nb_4.

The shell orbitals of Nb_4 along with its total and partial DOS are displayed in Figure S7 of the Supporting Information. As expected, the electrons in the 5s and 4d orbitals mostly contribute to the total DOS in the valence band (from −5.7 to −3.6 eV). Twenty valence electrons in Nb_4 with an ideal tetrahedral geometry constitute a ground configuration of $1a_1^2 2a_1^2 e^4 1t_2^6 2t_2^6$. These MOs correspond to the shell orbitals assigned as 1S, 2S, 1D, and 1P. In a tetrahedral field, the 1D shell splits into two sublevels t_2 and e. The former includes $1d_{xy}$, $1d_{yz}$, and $1d_{xz}$, while the latter includes $1d_{z^2}$ and $1d_{x^2-y^2}$. Three orbitals t_2 are higher in energy than the e orbitals, but they are somewhat lower than 1P orbitals. The electronic configuration of Nb_4 within the shell model is as follows: $1s^2 2s^2 1d_{z^2}^2 1d_{x^2-y^2}^2 1d_{xy}^2 1d_{yz}^2 1d_{xz}^2 1p_x^2 1p_y^2 1p_z^2$. The cluster exhibits a closed shell of electrons, and it thus is magic which is manifested in its higher thermodynamic stability.

Figure S8 of the Supporting Information describes the DOS of the Nb_6 cluster in D_{2h} structure and Figure S5 of the Supporting Information is that of the Nb_6 cluster in C_{2v} shape. In the dimer-capped rhombus form (C_{2v}, $^3B_2$), the contribution to the LUMO of s orbitals and p orbitals is approximately equal. Meanwhile, the role of s electrons (and p electrons) in the valence band is not as crucial as that of d electrons. For the Nb_6 with distorted octagon structure (D_{2h}, $^3B_{1u}$), the d orbitals mainly contribute to the total DOS in the valence band and the band gap.

4. Concluding Remarks

We reinvestigate in the present theoretical study the geometrical, electronic, and vibrational properties of a series of small niobium clusters in the range from two to six atoms using both DFT and CCSD(T) calculations, in conjunction with the pseudopotential basis sets cc-pV*a*Z-PP. Our results show that various lower lying states of these clusters are very close in energy, in such a way that their ground electronic states cannot unequivocally be established. As in many other transition metal clusters, niobium clusters tend to prefer multicoordinated geometries. The most stable trimeric form is thus triangular, not linear. The clusters containing more than three atoms exhibit already 3D shape in their most stable structures. The ground state of clusters with an odd number of electrons is usually a low spin, i.e. doublet, state. In contrast, neutral and cationic clusters with an even number of electrons tend to possess a high spin in the ground state, i.e. triplet state. Exceptions are the Nb_2^+ cation and the Nb_4 neutral. The Nb_2^+ dimer does not favor a low spin state whereas the neutral Nb_4 prefers a low spin arrangement (T_d, $^1A_1$). For anions, there is a competition between the lowest lying singlet and triplet states in clusters having an even number of electrons. Nevertheless, no simple rule can unambiguously be drawn for anions. Due to the closed electronic shells, the 10 (Nb_2) and 20 (Nb_4) electron systems are observed to be more thermodynamically stable than their neighbors.

We reevaluate the electron affinities, ionization energies, and IR spectra. Comparison with experimental IR results allows some new assignment for the Nb_5 and Nb_6 systems to be proposed. Although the pure functionals selected in this work appear to provide us with reliable spectroscopic information, the properties of some clusters remain extremely sensitive with the methods employed.

Acknowledgment. The authors are indebted to the K. U. Leuven Research Council for continuing support (GOA, IDO, and IUAP programs). P.V.N. thanks the Cantho University for a scholarship. M.T.N. thanks the ICST for supporting his stays in Vietnam. We are sincerely grateful to Dr. Andre Fielicke from the Fritz-Haber Institute, Berlin, for providing us with the original plots of his experimental IR spectra reported in ref 10.

Supporting Information Available: Complete ref 26 along with additional tables and figures as discussed in the text. This material is available free of charge via the Internet at http://pubs.acs.org.

References and Notes

(1) Schmid, G. *Adv. Eng. Mater.* **2001**, *3*, 737.
(2) Loh, S. K.; Lian, L.; Armentrout, P. B. *J. Am. Chem. Soc.* **1989**, *111*, 91–3168.
(3) Knickelbein, M. B.; Yang, S. *J. Chem. Phys.* **1990**, *93*, 1476–5760.
(4) Hales, D. A.; Lian, L.; Armentrout, P. B. *Int. J. Mass Spectron Ion Processes* **1990**, *102*, 269.
(5) Knickelbein, M. B.; Menezes, W. J. C. *Phys. Rev. Lett.* **1992**, *69*, 1046.
(6) Menezes, W. J. C.; Knickelbein, M. B. *J. Chem. Phys.* **1993**, *98*, 1856.
(7) Collings, B. A.; Athanassenas, K.; Rayner, D. M.; Hackett, P. A. *Z. Phys. D: At. Mol. Clusters* **1993**, *26*, 36.
(8) James, A. K.; Kowalczyk, P.; Fournier, R.; Simard, B. *J. Chem. Phys.* **1993**, *99*, 8504.
(9) Fielicke, A.; Ratsch, C.; Von Helden, G.; Meijer, G. *J. Chem. Phys.* **2005**, *122*, 091105.
(10) Fielicke, A.; Ratsch, C.; Von Helden, G.; Meijer, G. *J. Chem. Phys.* **2007**, *127*, 234306.
(11) Kietzmann, H.; Morenzin, J.; Bechthold, P. S.; Ganteför, G.; Eberhardt, W.; Yang, D. S.; Hackett, P. A.; Fournier, R.; Pang, T.; Chen, C. *Phys. Rev. Lett.* **1996**, *77*, 4528.
(12) Kietzmann, H.; Morenzin, J.; Bechthold, P. S.; Gantefor, G.; Eberhardt, W. *J. Chem. Phys.* **1998**, *109*, 2275.
(13) Wrigge, G.; Hoffmann, M. A.; Von Issendorff, B.; Haberland, J. *Eur. Phys. J. D* **2003**, *24*, 23.
(14) Zhai, H. J.; Wang, B.; Huang, X.; Wang, L. S. *J. Phys. Chem. A* **2009**, *113*, 3866.
(15) Goodwin, L.; Salahub, D. R. *Phys. Rev. A* **1993**, *47*, R774.
(16) Gronbeck, H.; Rosen, A. *Phys. Rev. B* **1996**, *54*, 1549.

(17) Gronbeck, H.; Rosen, A.; Andreoni, W. *Phys. Rev. A* **1998**, *58*, 4630.
(18) Fournier, R.; Pang, T.; Chen, C. *Phys. Rev. A* **1998**, *57*, 3683.
(19) Fowler, J. E.; Garcia, A.; Ugalde, J. M. *Phys. Rev. A* **1999**, *60*, 3058.
(20) Balasubramanian, K.; Zhu, X. L. *J. Chem. Phys.* **2001**, *114*, 10375.
(21) Kumar, V.; Kawazoe, Y. *Phys. Rev. B* **2002**, *65*, 125403.
(22) Majumdar, D.; Balasubramanian, K. *J. Chem. Phys.* **2001**, *115*, 885.
(23) Majumdar, D.; Balasubramanian, K. *J. Chem. Phys.* **2003**, *119*, 12866.
(24) Majumdar, D.; Balasubramanian, K. *J. Chem. Phys.* **2004**, *121*, 4014.
(25) Janssens, E.; Neukermans, S.; Lievens, P. *Curr. Opin. Solid State Mater. Sci.* **2004**, *8*, 185.
(26) Frisch, M. J. *Gaussian 03*, revision B.03; Gaussian, Inc., Wallingford, CT, 2003. The full reference is given in the Supporting Information.
(27) Werner, H. J., *MOLPRO*, Version 2009.2, a package of ab initio programs.
(28) Peterson, K. A. *J. Chem. Phys.* **2003**, *119*, 11099.
(29) Peterson, K. A.; Figgen, D.; Goll, E.; Stoll, H.; Dolg, M. *J. Chem. Phys.* **2003**, *119*, 11113.
(30) Peterson, K. A.; Puzzarini, C. *Theor. Chem. Acc.* **2005**, *114*, 283.
(31) Roos, B. O.; Lindh, R.; Malmqvist, P. A.; Veryazov, V.; Widmark, P. O. *J. Phys. Chem. A* **2005**, *109*, 6575.
(32) Iseda, M.; Nishio, T.; Han, S. Y.; Yoshida, H.; Terasaki, A.; Kondow, T. *J. Chem. Phys.* **1997**, *106*, 2182.
(33) Gronbeck, H.; Rosen, A. *J. Chem. Phys.* **1997**, *107*, 10620.
(34) Tenderholt, A. *PyMOlyze-2.0*; Stanford University, Stanford, CA, 2005.

JP103484K